Optik - International Journal for Light and Electron Optics 207 (2020) 163848

Contents lists available at ScienceDirect

Optik

journal homepage: www.elsevier.com/locate/ijleo

Original research article

# Research on beam quality improvement method of LD side-pumped acousto-optic Q-Switched anisotropic Nd:YLF laser

Wu Rina, Fan Yang, Jiaqi Lu, Nan Zhang, Songming Guo, Yeqiu Li, Yue Zhang, Dai Qin*

*School of Science, Shenyang Ligong Unibersity, Shenyang 110159, China*

ARTICLE INFO

*Keywords:*
Anisotropic Nd: YLF crystal
Thermal strain distribution
Gaussian aperture
Improve beam quality

ABSTRACT

In order to achieve a high beam quality for acousto-optic Q-switched anisotropic Nd:YLF quasi-continuous lasers, the influence factors of Nd:YLF laser beam quality is studied. The thermal strain distribution of an anisotropic Nd:YLF laser is simulated by finite element method in steady state, the laser beam is optimized by inserting a Gaussian aperture into the resonator cavity, and the distribution of the light field in the resonator is analyzed according to the Collins theory. The beam quality with or without a Gaussian aperture in the resonant cavity is experimentally compared. Experiments show that inserting a Gaussian aperture in the resonant cavity can effectively improve the output beam quality for anisotropic Nd:YLF lasers.

## 1. Introduction

As a laser gain medium pumped by a laser diode (LD), Nd:YLF crystals are indispensable laser crystals due to their unique properties [1–4]. Compared to Nd:YAG crystals, Nd:YLF crystals have twice the fluorescence lifetime, twice the energy storage. Under the same pumping conditions, a Nd:YLF laser owns a lower laser threshold than a Nd:YAG laser [5]. In addition, the Nd:YLF laser presents a weaker thermal lensing effect because the negative temperature coefficient of the refractive index of the Nd:YLF crystal produces a negative thermal lens effect and counteracts the optical path variation caused by the expansion of the crystal clear surface [6].

However, the anisotropic of the thermal expansion coefficient of the Nd:YLF crystal will lead to an uneven stress distribution of thermal effect in the crystal. As a result, the uneven thermal stain of the crystal will result in a low laser beam quality. In 2007, Ma et al. conducted a numerical study on the thermal stress effect of diode-end-pumped Nd:YLF plate laser crystals, in which an accurate numerical solution is obtained based on the theoretical model using the three-dimensional finite element analysis. After analyzing the thermal fracture damage of the Nd:YLF slab under the lasering and non-lasering conditions, they concluded that the large thermal stress causes large fracture damage to Nd:YLF crystal [7]. In 2012, Huang et al. used the natural birefringence of the Nd:YLF crystal to achieve a reliable TEM00-mode linearly polarized laser at 1053 nm in a compact concave-plano resonator [8]. In 2016, Zhang et al. analyzed the thermal effect of Nd:YLF crystals with the finite element method, and experimentally verified this theoretical simulation result [9]. In 2017, AGMY et al. numerically simulated the thermal effect of Nd:YLF laser rods, and calculated the temperature and stress distributions of Nd:YLF laser rods by the finite element simulation method. The calculation results showed that the pump power of the laser bar can reach 40 W without thermal stress-induced cracks [10].

In this paper, the thermal effect and strain distribution of an anisotropic Nd:YLF crystal rod on the output laser beam are analyzed.

* Corresponding author.
*E-mail address:* daiqin2003@126.com (D. Qin).

https://doi.org/10.1016/j.ijleo.2019.163848
Received 10 September 2019; Accepted 20 November 2019
0030-4026/ 

In order to improve the laser beam quality, a Gaussian aperture is inserted into the laser resonant cavity. The spatial distribution of the output laser is theoretical simulated by Collins theory and experimental investigated. Both results demonstrate that the laser beam quality has been effectively improved with the help of the Gaussian aperture.

## 2. Theoretical simulation and analysis

### 2.1. Theoretical models of thermal effects

In an anisotropic crystal, the equation of the heat conduction is

$$\rho c\frac{\partial T}{\partial t} = K_{22}\frac{\partial^2 T(x,y,z)}{\partial x^2} + K_{33}\frac{\partial^2 T(x,y,z)}{\partial y^2} + K_{44}\frac{\partial^2 T(x,y,z)}{\partial z^2} + Q \tag{1}$$

where ρ is the density of the crystal, $c$ is the specific heat of the crystal, $K_{ii}$ is the heat conductivity, and $Q$ is the intensity.

$$Q = \frac{2qT_l}{cw_p{}^2}(1 - e^{-Td})^{-1}\exp[-\frac{2r^2}{w_p{}^2}]e^{-Tz} \tag{2}$$

where $q$ is the total heat, $T_l$ is the absorption coefficient of the medium, $w_p$ is the pump spot radius, and $d$ is the thickness of the laser crystal.

The circulating water cooling is performed on the side surface of the laser rod. The cooling boundary conditions can be expressed as follows :

$$\left.\frac{dT}{dr}\right|_{r=r_0} = \frac{h}{K}[T_c - T(r_0)] \tag{3}$$

where $h$ is the heat transfer coefficient, and $Tc$ is the temperature of the cooling liquid.

The stress distribution of the laser crystal is

$$\begin{cases} \sigma_x = -[Y\alpha_x/(1-v)]\Delta T_1 \\ \sigma_y = -[Y\alpha_y/(1-v)]\Delta T_2 \\ \sigma_z = v(\sigma_x + \sigma_y) - Y\alpha_z\Delta T_3 \end{cases} \tag{4}$$

where $Y$ is Young's modulus, $v$ is the Poisson's ratio, $q_v$ is the heat generation per unit volume, $\alpha_x$, $\alpha_y$ and $\alpha_z$ are coefficients of the thermal expansion in different directions, respectively, and $\Delta T$ is the temperature difference.

According to the Hook's law, the actual strain distribution of the laser crystal rod is

$$\begin{cases} \varepsilon_x = \frac{1}{E}[\sigma_x - v(\sigma_y + \sigma_z)] + \alpha_x\Delta T \\ \varepsilon_y = \frac{1}{E}[\sigma_y - v(\sigma_x + \sigma_z)] + \alpha_y\Delta T \\ \varepsilon_z = \frac{1}{E}[\sigma_z - v(\sigma_x + \sigma_y)] + \alpha_z\Delta T \end{cases} \tag{5}$$

The thermal effects of an acoustic-optic Q-switched Nd:YLF laser pumped on the side of LD are simulated via the equation of the heat conduction, in which the crystal size is $\Phi$ 4 × 80 mm$^3$ and the pump utilizes a triangular-shaped side-pump structure. Because the convective heat transfer coefficient of the two end faces of the laser crystal is much smaller than that of the side of the laser crystal, the cooling conditions of the two end faces of the laser crystal and air convection are ignored.And in the simulation, the direction parallel to c-axis of the crystal is defined as the Y-axis, and the direction perpendicular to axis c is defined as the X-axis (Table 1).

### 2.2. Analysis of simulated results

Fig.1 is the optical path diagram of the simulation experiment. In the theoretical simulation process, the crystal rod can be equivalent to a thermal lens with a certain focal length.

When the anisotropic Nd: YLF laser crystal reach a stable state(the crystal bar temperature doesn't change under theoretical simulation.), the laser crystal has the highest temperature at the center and a lower temperature at the edges. Because the pump source is arranged in a symmetrical triangular structure, the temperature of the laser crystal forms a triangular distribution.

The thermal strain distributions of anisotropic and isotropic laser crystals are compared by finite element analysis. As shown in Fig. 4, when the thermal expansion coefficient is isotropic, the strain trend along the x and y axes tends to be the same, and the strain distribution in both directions is symmetrical. The x and y strain distributions are same in the center of the crystal, whereas, have a small discrepancy around the edge of the crystal rod which caused by the uneven thermal strain distribution due to the symmetrical triangular structure of the pump source. When the thermal expansion coefficient is anisotropic, the x-axis strain is significantly larger than the Y-axis strain, and the closer to the edge of the crystal rod, the bigger the difference in thermal strain between the two directions. As a result, the overall deformation is asymmetric, which affects the output laser beam quality.

**Table 1**
The Nd:YLF crystal parameters.

| | |
|---|---|
| Specific heat capacity | 790 J/(kg℃) |
| Density | $3.99 \times 10^{-3}$ g/mm$^3$ |
| Heat conductivity | $6.3 \times 10^{-3}$ W/(mm*K) |
| Coefficient of thermal expansion | $13 \times 10^{-6}$ ℃$^{-1}$ (⊥c axis)<br>$8 \times 10^{-6}$ ℃$^{-1}$(‖c axis) |
| Poisson's ratio | 0.33 |
| Elasticity modulus | $7.5 \times 10^{10}$ N/m$^2$ |

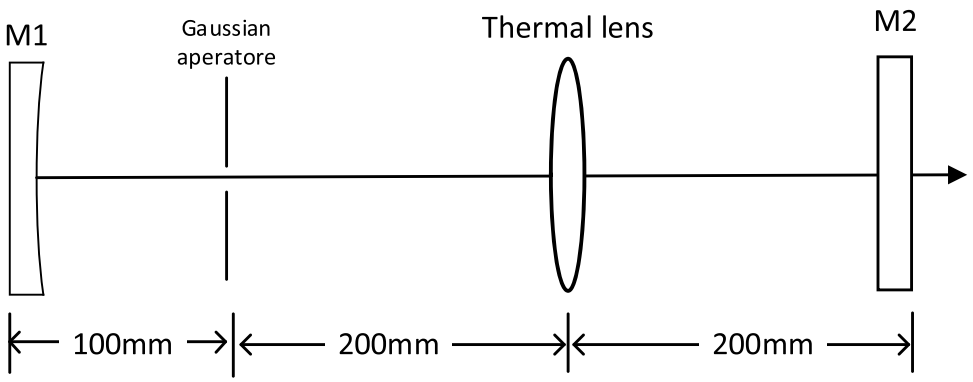


**Fig. 1.** Optical path diagram of the simulation experiment.

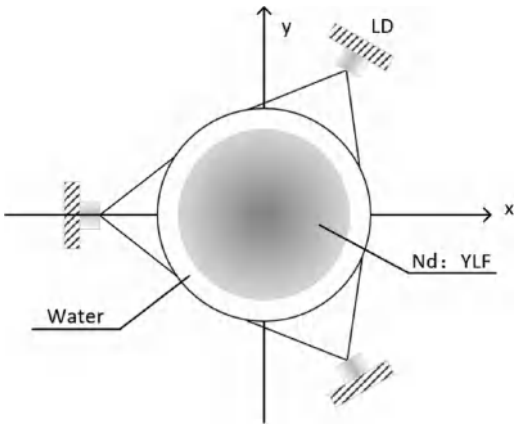


**Fig. 2.** Pump structure diagram.

## 3. The experimental device of laser

The schematic of the laser setup is shown in Fig. 2, in which the structure of the optical resonator is a plano-concave cavity.The cavity length is 50 cm. M1 is a plano-concave mirror with a curvature radius of 1 m and 1053 nm all-reflective (AR) film coating, and the output mirror M2 is a plane mirror with a transmittance T = 20 %. The Nd:YLF crystal with a size of Φ 4 × 80 mm$^3$ is cut along the a-axis. Three LD bars are symmetrically arranged around the crystal rod to achieve side pumping. Through the precise temperature control system LD pump source temperature control. The center operating frequency of the Acousto-optic Q-switch (GOOCH & HOUSEGO) is 27 MHz, the outer radius of the Gaussian aperture is 10 mm,the radius of the light spot on the film lf the Gaussian aperture is 4 mm. the working wavelength is 1047 −1064 nm, the working medium is molten silicon, and the transmittance > 99.8 %. The laser crystal and Acousto-optic Q crystal module are cooled by deionized water circulating cooling system, and the control temperature is kept at 21 ℃ (Fig. 3).

As shown in Fig. 5, the Gaussian aperture is placed between the mirror M1 and the crystal rod, the outer radius of the Gaussian aperture is 10 mm, the radius of the light spot on the film of the Gaussian aperture is 4 mm. The spot distribution of the output laser with or without a Gaussian aperture is measured by a beam quality analyzer(Spiricon, BM-USB-SP620) outside of the resonator.

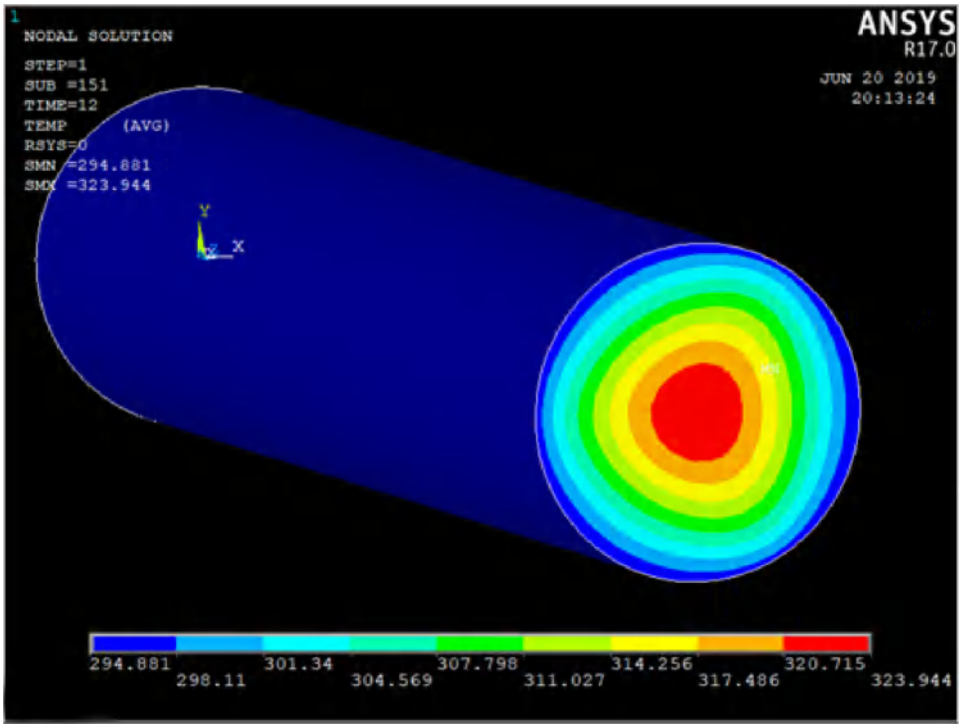


**Fig. 3.** Temperature distribution.

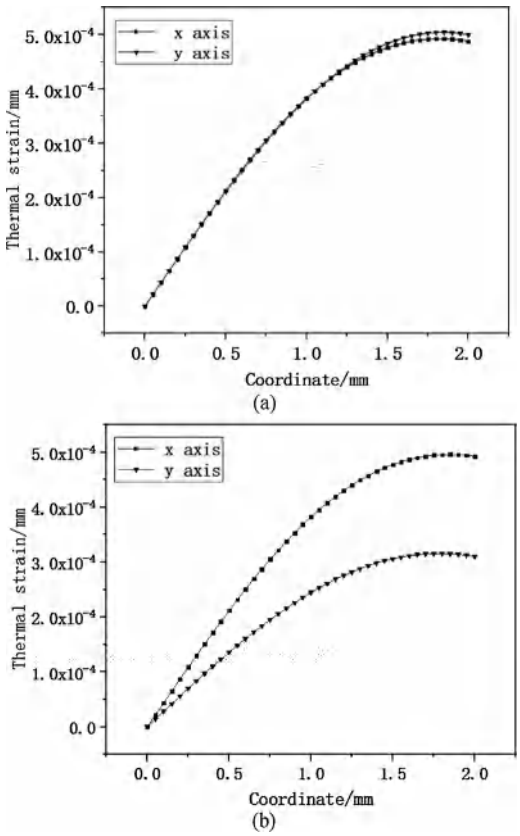


**Fig. 4.** Nd:YLF crystal strain comparison: (a) Isotropic crystal strain. (b) Anisotropic crystal.

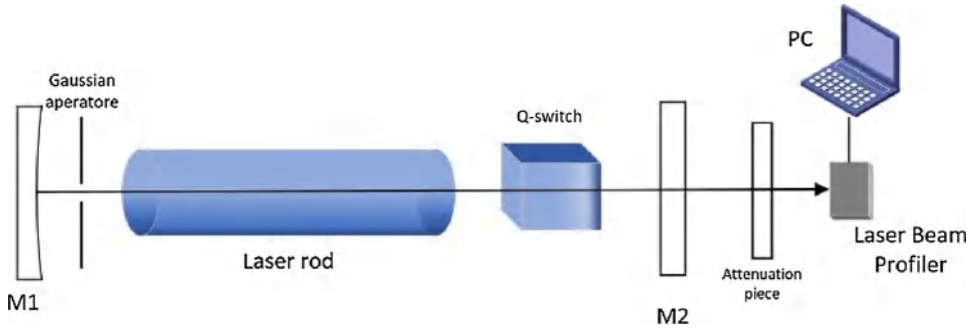


**Fig. 5.** Schematic of laser experimental setup.

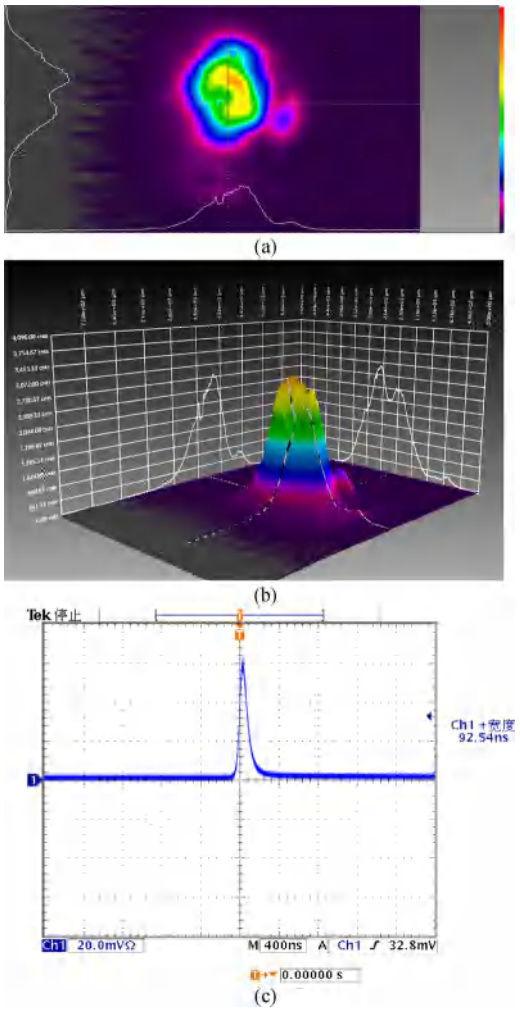


**Fig. 6.** Profiles of a laser output beam without a Gaussian aperture: (a) Two-dimensional distribution of the output beam profile and pattern (b) Three-dimensional distribution of the output beam profile and pattern(c)Pulse width figure.

## 4. Experimental results and analysis

The distribution of the output laser spot of the Acousto-optic Q-switched Nd:YLF laser without a Gauss aperture is presented in Fig. 6.The laser beam diameter is about 1.8 mm and the wavelength of the output beam is 1053 nm,the repetition rate is 1 kHz.,the pulse width is 92.54 nm.The overall profile of the output beam is not uniform, high-order modes appear at the edge of the spot, and the beam quality is poor.

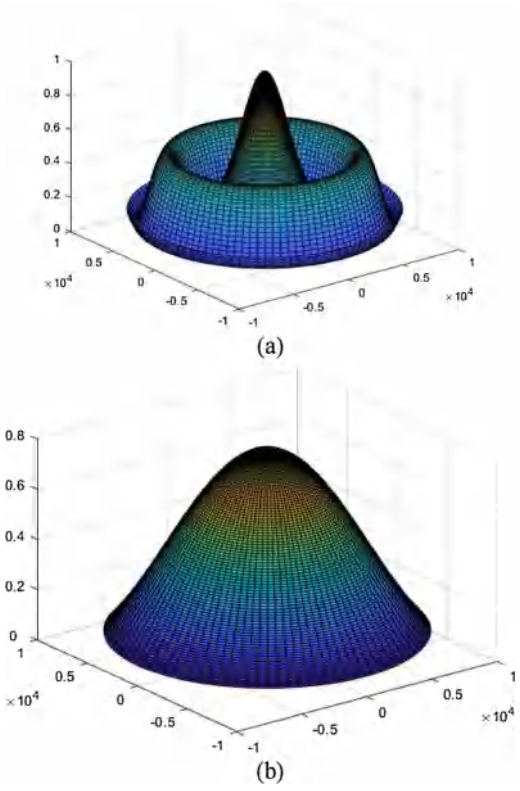


**Fig. 7.** The beam mode distribution of output laser: (a) Without a Gaussian aperture. (b) With a Gaussian aperture.

According to the Collins formula [11], the mode distribution of the laser beam in a Cartesian coordinate system can be expressed as:

$$U(x, y) = -\frac{iexp(ikl)}{\lambda B}\iint_S U(r_1, r_2)exp\left(\frac{ik}{2B}[A(r_1^2 + r_2^2) + D(x^2 + y^2) - 2(r_1x + r_2y)]\right)dr_1dr_2 \quad (6)$$

where $l$ is the length of the resonator, $k$ is the wavenumber, and $A$, $B$, $C$ and $D$ are one-way matrix elements of the Optical system transformation matrix.

The simulated facula in a Gauss aperture-based resonator cavity using Collins theory is shown in Fig. 7. When the Gaussian aperture is inserted into the resonator cavity, the mode distribution of the laser output beam is improved and a stable fundamental mode output is achieved.

The experimental facula in a Gaussian aperture-based resonator cavity is measured with a beam quality analyzer and shown in Fig. 8 and the laser beam diameter is about 1.2 mm.The overall profile of the facula is uniform, the edge is smooth, and the mode distribution is good. The higher-order modes are effectively suppressed, and the optical quality is significantly controlled.

Fig. 9 shows the out put power dependence on the pump current when a Gaussian aperture is inserted into the resonant cavity.

Due to the gaussian aperture is inserted into the resonant cavity, the loss in the cavity increase, and the output power decrease. The maximum output power of the laser is 2.51 W at the pump current is 18A.

## 5. Conclusions

The thermal strain distribution of the Nd:YLF crystal is not uniform due to the anisotropy of the thermal expansion coefficient, which induces a poor beam quality of the Nd:YLF laser. In this paper, the thermal effect and strain distribution of an Acousto-optic Q-switched Nd:YLF crystal in a plano-concave cavity are studied, and the theoretical simulation is performed using a finite element analysis method. The simulated results show that the anisotropy of the Nd:YLF crystal will result in an uneven strain distribution and higher order modes of output laser which is also verified by experimental results. In order to improve the beam quality, a Gaussian aperture is inserted into the resonant cavity. The experimental results demonstrate that the Gaussian diaphragm can effectively suppress the generation of higher-order modes, obtain a better laser beam quality.

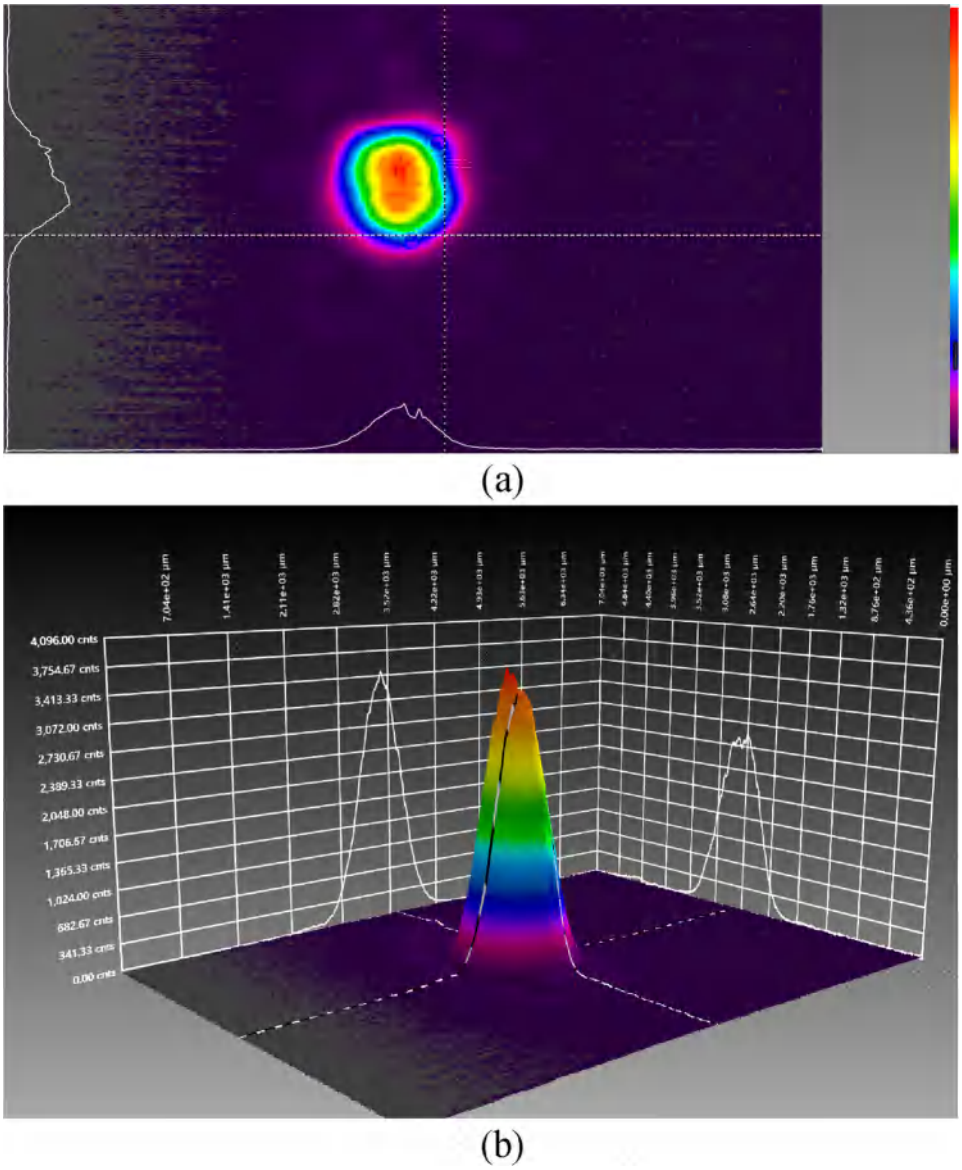


**Fig. 8.** Laser output beam spot with Gaussian aperture : (a) Two-dimensional distribution of the output beam profile and pattern (b) Three-dimensional distribution of the output beam profile and pattern.

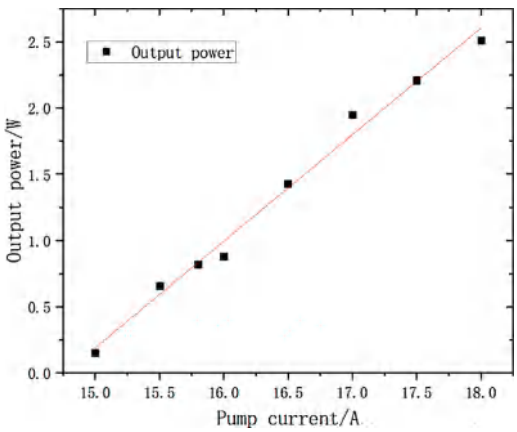


**Fig. 9.** Dependence of the output power on the pump current.

## Acknowlegment

This work is supported by the National Natural Science Foundation of China (No.61705145), Program for Liaoning Innovative Talents in University (No.LR2016079), Natural Science Foundation of Liaoning Province (No.20180550330).

## References

[1] W. Koechner, Solid-state Laser Engineering, Springer, 2013.
[2] Y. Wei, S. Xu, C.H. Huang, W.D. Chen, F.J. Zhuang, L.X. Huang, Z.Q. Chen, G. Zhang, J. Opt. 14 (2012) 095201.
[3] A. Schellhorn Hirth, C. Kieleck, C. Kieleck, Opt. Lett. 28 (2003) 1933.
[4] A.K. Cousins, IEEE J. Quantum Electron. 28 (2002) 1057.
[5] T.T. Lu, J.T. Wang, M.J. Huang, D. Liu, X.L. Zhu, Chinese Opt. Lett. 10 (2012) 36.
[6] P.J. Hardman, W.A. Clarkson, G.J. Friel, M. Pollnau, D.C. Hanna, IEEE J. Quantum Electron. 35 (1999) 647.
[7] Z. Ma, J.C. Gao, D.J. Li, J.L. Li, N.L. Wu, K.M. Du, Opt. Commun. 281 (2008) 3522.
[8] Y.J. Huang, C.Y. Tang, W.L. Lee, S.C. Huang, Y.F. Chen, Applied Physics B 108 (2012) 313.
[9] Z.L. Zhang, Q. Liu, M.M. Nie, E.C. Ji, M.L. Gong, Applied Physics B 120 (2015) 689.
[10] R.M. El-Agmy, N. Al-Hosiny, Photonic Sens. 7 (2017) 1.
[11] Q. Dai, S.C. Zhang, Y.Q. Li, J.F. Cui, R.B. Ning, R.N. Wu, Opt. – Int. J. Light Electron. Opt. 176 (655) (2019).